



Joint sensing methods to reconstruct acoustic fields over space

Verburg Riezu, Samuel Arturo; Fernandez Grande, Efren

Published in:
Proceedings of InterNoise20

Publication date:
2021

Document Version
Peer reviewed version

[Link back to DTU Orbit](#)

Citation (APA):
Verburg Riezu, S. A., & Fernandez Grande, E. (2021). Joint sensing methods to reconstruct acoustic fields over space. In *Proceedings of InterNoise20* (pp. 3699-3706). Institute of Noise Control Engineering.

General rights

Copyright and moral rights for the publications made accessible in the public portal are retained by the authors and/or other copyright owners and it is a condition of accessing publications that users recognise and abide by the legal requirements associated with these rights.

- Users may download and print one copy of any publication from the public portal for the purpose of private study or research.
- You may not further distribute the material or use it for any profit-making activity or commercial gain
- You may freely distribute the URL identifying the publication in the public portal

If you believe that this document breaches copyright please contact us providing details, and we will remove access to the work immediately and investigate your claim.



Joint sensing methods to reconstruct acoustic fields over space

Samuel A. Verburg¹

Acoustic Technology, Department of Electrical Engineering, Technical University of Denmark
Ørsteds Plads, building 352, 2800 Kongens Lyngby, Denmark

Efren Fernandez-Grande²

Acoustic Technology, Department of Electrical Engineering, Technical University of Denmark
Ørsteds Plads, building 352, 2800 Kongens Lyngby, Denmark

ABSTRACT

Optical interferometry makes it possible to measure acoustic fields, by exploiting the acousto-optic interaction, without using microphones or other electroacoustic transducers. Scanning interferometers can sample a sound field with high spatial resolution in an automated way. Therefore, optical interferometry is particularly suitable for measuring sound fields over space at mid and high frequencies, where sampling requirements make the use of microphones demanding and costly. However, optical methods are sensitive to vibrations of the equipment that biases the measurements, especially at low frequencies. In this study we propose a joint sensing approach that combines data acquired with conventional microphones as well as with an optical interferometer. The robustness and qualitative accuracy at low frequencies is improved due to the microphone data, whereas the sound field at higher frequencies is successfully captured over space with the scanning interferometer. In an experimental study, a three dimensional acoustic field is sampled combining the two sensing methods. The results show that the frequency range in which the reconstruction is correct is extended using the joint microphone-interferometer measurements.

1. INTRODUCTION

The spatial properties of acoustic fields are typically captured using microphone arrays or networks of sensors [1–3]. In recent decades an alternative sensing principle has been explored, which makes use of the acousto-optic interaction to acquire acoustic data over space. The acousto-optic interaction describes the perturbations on the propagation of light induced by pressure waves. Acousto-optic sensing methods can sample pressure fields by measuring the acoustically induced perturbations on laser beams emitted by an optical interferometer [4–13]. Recently, an acousto-optic approach has been presented that enables to measure arbitrary sound fields volumetrically, based on a set of non-uniform beam projections [14, 15].

Scanning interferometers can accurately direct a sensing laser beam in multiple directions with a very fine resolution using a set of moving mirrors, which enables to scan pressure fields over space in an automated way. The high spatial resolution achieved by scanning interferometers makes acousto-optic sensing especially suitable to capture volumetric sound fields at mid and high frequencies, where

¹saveri@elektro.dtu.dk

²efg@elektro.dtu.dk

the use of microphone arrays would be intractable. However, the acousto-optic interaction is a fairly weak phenomenon, and its measurement using interferometers is sensitive to self-noise and vibration of the equipment, which are particularly problematic at low frequencies [15, 16].

In this study we present a fused sensing methodology to combine acoustic information from data acquired via different sensing paradigms. We examine the combination of pressure measurements (acquired with a conventional pressure microphone) and optical measurements (obtained with an optical interferometer). The pressure measurements are used to sample the sound field at low frequencies, and to increase the robustness and quantitative accuracy of the reconstruction. This is particularly valuable when the optical measurements are corrupted by low frequency noise and other sources of error. The high spatial resolution achieved by the optical interferometer enables to capture the volumetric sound field at higher frequencies. In addition to pressure and optical measurements, the proposed fused sensing formulation makes it possible to include other sources of acoustic information, e.g. particle velocity measurements, in the reconstruction problem. In an experimental study we sample and reconstruct the sound field inside the volume of a room using the proposed fused sensing approach. The results show that the combination of sensing principles can extend considerably the operational frequency range, in comparison to the case where pressure and optical measurements are used independently.

2. THEORY

A plane wave expansion of the sound field $p(\mathbf{r})$, where $\mathbf{r} = (x, y, z)$, corresponds to

$$p(\mathbf{r}) = \sum_{n=1}^N X_n e^{j\mathbf{k}_n \cdot \mathbf{r}}, \quad (1)$$

where X_n^p is the complex coefficient and \mathbf{k}_n is the wavenumber vector associated with the n^{th} plane wave in the expansion. The operator (\cdot) indicates the dot product $\mathbf{k} \cdot \mathbf{r} = k_x x + k_y y + k_z z$. If pressure measurements are acquired with a microphone at M locations, Eq. 1 can be written algebraically as

$$\mathbf{b}_p = \mathbf{H}_p \mathbf{x} + \mathbf{e}_p, \quad (2)$$

where $\mathbf{b}_p \in \mathbb{C}^{M \times 1}$ is a vector containing the pressure measurements $p(\mathbf{r}_m)$. The sensing matrix $\mathbf{H}_p \in \mathbb{C}^{M \times N}$ contains the exponential terms $e^{j\mathbf{k}_n \cdot \mathbf{r}_m}$, and $\mathbf{x} \in \mathbb{C}^{N \times 1}$ is the vector of complex coefficients X_n . The vector $\mathbf{e}_p \in \mathbb{C}^{M \times 1}$ accounts for the noise present in the measurements, here assumed independent and with identical normal distribution with zero-mean [17]. An estimate of the plane wave complex coefficients can be obtained by solving

$$\hat{\mathbf{x}}_p = \arg \min \left\{ \|\mathbf{H}_p \mathbf{x} - \mathbf{b}_p\|_2^2 + \lambda \|\mathbf{x}\|_2^2 \right\} \quad (3)$$

where λ is the regularization parameter. The solution of the minimization problem of Eq. (3) corresponds to a conventional regularized pseudo-inversion [18].

A plane wave expansion based on optical interferometer measurements can be performed in a similar manner [14, 15],

$$v(s) \approx \frac{1}{n_0} \frac{\partial n}{\partial p} j\omega \sum_{n=1}^N X_n^v \int_S e^{j\mathbf{k}_n \cdot \mathbf{r}} ds, \quad (4)$$

where s is an integration variable along the path followed by the sensing laser beam sent by the interferometer, $\frac{\partial n}{\partial p}$ is the piezo-optic coefficient of the medium [4, 9], and n_0 is the speed of light in the unperturbed medium. Measurements with a number L of sensing laser beams lead to the corresponding system of equations

$$\mathbf{b}_v = \mathbf{H}_v \mathbf{x} + \mathbf{e}_v, \quad (5)$$

where the L interferometer measurements are stacked in $\mathbf{b}_v \in \mathbb{C}^{L \times 1}$, the elements of the sensing matrix $\mathbf{H}_v \in \mathbb{C}^{L \times N}$ are

$$\mathbf{H}_v(\mathbf{k}_n, s_l) = \frac{1}{n_0} \frac{\partial n}{\partial p} j\omega \int e^{j\mathbf{k}_n \cdot \mathbf{r}} ds_l,$$

and the vector $\mathbf{e}_v \in \mathbb{C}^{L \times 1}$ contains the noise.

In addition to the sound pressure measurements and the laser projections, the particle velocity of the sound field can also be incorporated into the problem. This particle velocity can be either measured with a velocity sensor [19], or prescribed at given points of the domain, for example on the boundary of a rigid surface [20]. The plane wave expansion based on particle velocity is written algebraically as

$$\mathbf{b}_u = \mathbf{H}_u \mathbf{x} + \mathbf{e}_u, \quad (6)$$

where $\mathbf{b}_u \in \mathbb{C}^{K \times 1}$ is the vector containing the K particle velocity measurements. The sensing matrix $\mathbf{H}_u \in \mathbb{C}^{K \times N}$ has elements $\frac{1}{j\omega\rho} \nabla_{\mathbf{n}} e^{j\mathbf{k}_n \cdot \mathbf{r}}$, where \mathbf{n} is the direction of the measured particle velocity vector. The vector $\mathbf{e}_u \in \mathbb{C}^{K \times 1}$ contains the noise.

These three sensing principles (pressure, optical and particle velocity measurements) can be combined in one single system

$$\mathbf{W}_c \begin{bmatrix} \mathbf{b}_p \\ \mathbf{b}_v \\ \mathbf{b}_u \end{bmatrix} = \mathbf{W}_c \begin{bmatrix} \mathbf{H}_p \\ \mathbf{H}_v \\ \mathbf{H}_u \end{bmatrix} \mathbf{x} + \mathbf{W}_c \begin{bmatrix} \mathbf{e}_p \\ \mathbf{e}_v \\ \mathbf{e}_u \end{bmatrix}, \quad (7)$$

where

$$\mathbf{W}_c = \begin{bmatrix} \mathbf{W}_p & 0 & 0 \\ 0 & \mathbf{W}_v & 0 \\ 0 & 0 & \mathbf{W}_u \end{bmatrix}$$

and $\mathbf{W}_p \in \mathbb{C}^{M \times M}$, $\mathbf{W}_v \in \mathbb{C}^{L \times L}$, and $\mathbf{W}_u \in \mathbb{C}^{K \times K}$ are scaling matrices. It is necessary to apply a scaling when combining acoustic data from different sensing principles since their energy might differ by several orders of magnitude (e.g. the ratio between the amplitudes of \mathbf{b}_v and \mathbf{b}_p is typically of the order of 10^{-7} , and the ratio between \mathbf{b}_u and \mathbf{b}_p is of the order 10^{-3}). The scaling improves the conditioning of the problem and avoids an excessive weight of one of the measurements systems [21]. In this study we choose $\mathbf{W}_p = \|\mathbf{b}_p\|_2^{-1} \mathbf{I}^M$, $\mathbf{W}_v = \|\mathbf{b}_v\|_2^{-1} \mathbf{I}^L$, and $\mathbf{W}_u = \rho c \|\mathbf{b}_p\|_2^{-1} \mathbf{I}^K$, where \mathbf{I}^M , \mathbf{I}^L , \mathbf{I}^K are the $M \times M$, $L \times L$, and $K \times K$ identity matrices, ρ is the air density air and c is the sound speed. The plane wave coefficients estimated from the combination of measurements is

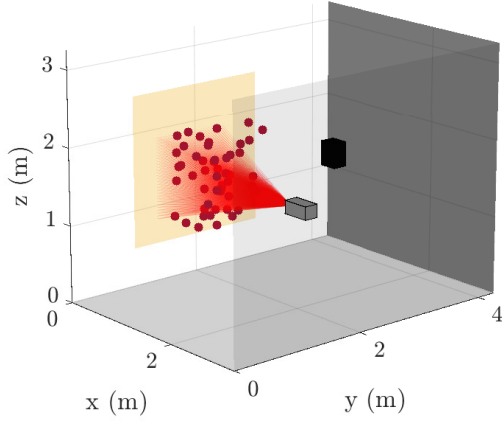
$$\hat{\mathbf{x}}_c = \arg \min \left\{ \|\mathbf{W}_c(\mathbf{H}_c \mathbf{x} - \mathbf{b}_c)\|_2^2 + \lambda \|\mathbf{x}\|_2^2 \right\} \quad (8)$$

where $\mathbf{H}_c = [\mathbf{H}_p \mathbf{H}_v \mathbf{H}_u]^T$ and $\mathbf{b}_c = [\mathbf{b}_p \mathbf{b}_v \mathbf{b}_u]^T$. Once the plane wave coefficient are estimated, the pressure at any position \mathbf{r}_r in the measured domain can be computed by multiplying $\hat{\mathbf{x}}_c$ with the corresponding reconstruction matrix \mathbf{H}_r , with elements $e^{j\mathbf{k}_n \cdot \mathbf{r}_r}$.

Equation 8 implicitly assumes that the scaled error terms $\mathbf{W}_p \mathbf{e}_p$, $\mathbf{W}_v \mathbf{e}_v$, and $\mathbf{W}_u \mathbf{e}_u$ are uncorrelated and have covariance matrix $\sigma^2 \mathbf{I}^{(M+L+K)}$. If an estimate of the covariance matrices of the different sensing systems is available, an alternative scaling that accounts for the different noise levels of the sensing principles can be done [18].

3. EXPERIMENTAL STUDY

The proposed fused sensing method is tested in an experimental study. The sound field inside an empty room was sampled using pressure measurements with a microphone, and optical measurements acquired with a scanning interferometer (see the setup in Figs. 1a and 1b). The room, with dimensions $3.173 \times 4.276 \times 3.249$ m, has concrete walls, floor and ceiling. For this experiment



(a) Figure 1a: Sketch of the experimental setup. Black cube: loudspeaker. Gray cube: laser vibrometer. Red dots: position of pressure measurements. Yellow: surface at which the normal component of the particle velocity is prescribed to be zero.



(b) Figure 1b: Photograph of the experimental setup.

two of the walls and the floor were covered with acoustically absorptive material (gray areas in Fig. 1a). The reverberation time of the room is between 0.7 and 1.4 s in the octave bands between 125 and 2000 Hz. A Dynaudio BM6 loudspeaker was placed in one of the room corners (see black cube in Fig. 1a), and the room frequency responses were measured using pseudo-random noise. A total of $L = 841$ optical measurements were automatically acquired using a scanning Laser Doppler Vibrometer (LDV) (its position indicated by the gray box in Fig. 1a). The scanning sequence of 841 points took approximately 12 hours to complete and it was performed in an automated way without any intervention. Scanning LDVs are compact interferometers normally used to measure vibration velocity. In this study, however, the laser beams (red lines in Fig. 1a) were directed towards one of the rigid walls in order to measure the acousto-optic effect in the medium, and not the surface vibration of an object. The vibration velocity of the LDV unit was monitored using a charge accelerometer, which showed that the optical measurements were corrupted by vibration noise below approx. 1 kHz. A high-pass filter with the cut-off at 1 kHz was therefore applied to the LDV output, and the scaling matrix \mathbf{W}_v in Eq. (7) was set to 0 for frequencies below 1 kHz. A total of 160 pressure measurements were acquired with a 1/2 inch measurement microphone. The positions of the microphone were chosen within and around the volume covered by the optical scan. A number $M = 50$ of the 160 pressure measurements (see red dots in Fig. 1a) were randomly chosen for the estimation of the wave coefficients (these pressure measurements correspond to \mathbf{b}_p in Eqs. (2) and (7)). The other 110 measurements (not shown in Fig. 1a) were used as a reference to assess the validity of the reconstruction. Additionally, particle velocity information was included by prescribing it at given points in the domain. The surface scanned by the LDV $\partial\Omega$ is assumed to be rigid, and therefore the vector component of the acoustic particle velocity normal to this surface is zero ($\mathbf{b}_u(\mathbf{n}_{\partial\Omega}, \mathbf{r}_{\partial\Omega}) = 0$, where $\mathbf{n}_{\partial\Omega} \perp \partial\Omega$ and $\mathbf{r}_{\partial\Omega} \in \partial\Omega$). [20] In this experiment we prescribe the component of the particle velocity normal to the yellow surface in Fig. 1a to be zero.

Figure 2 shows the pressure level at a single position between 50 and 2000 Hz. The solid black curve corresponds to the pressure measured with a microphone, which constitutes the reference. The dotted red curve corresponds to the reconstructed pressure using exclusively the $M = 50$ pressure measurements (red dots in Fig. 1a), i.e. this reconstruction is the solution to Eqs. (2) and (3). The dashed blue curve indicates the reconstructed pressure using exclusively the optical measurements (red lines in Fig. 1a), i.e. this reconstruction corresponds to the solution of Eq. (5). The solid

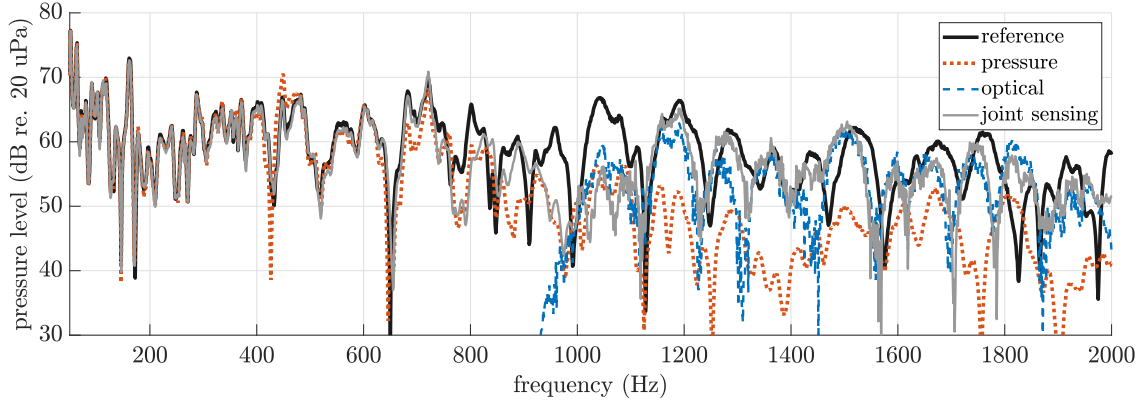


Figure 2: Sound pressure level across frequency at position (0.148, 1.471, 1.132) m. Solid black: reference pressure measured with a microphone. Dotted red: reconstructed pressure by the pressure measurements exclusively. Dashed blue: reconstructed pressure by the optical measurements exclusively. Solid gray: reconstructed pressure by the proposed fused sensing approach (combines pressure, optical and particle velocity information).

gray curve shows the reconstructed pressure achieved when combining pressure, optical and particle velocity measurements (red dots, red lines and yellow surface in Fig. 1a), i.e. this reconstruction is the solution of the fused sensing approach of Eqs. (7) and (8). At low frequencies, below 400 Hz, the proposed fused sensing approach (solid gray line in Fig. 2) achieves an almost perfect reconstruction. At this frequencies the sound field is rather uniform over space, and a small number of pressure measurements combined with the particle velocity information normal to the scanned surface suffices to capture the its spatial features. The reconstruction using exclusively pressure measurements (dotted red curve in Fig. 2) is also successful in this frequency range. Between 400 and 800 Hz, the fused sensors are able to accurately recover the sound field, with some deviations around 800 Hz when compared with the reference pressure measurement (solid black curve in Fig. 2). In this frequency range the proposed approach outperforms the pressure-based reconstruction, especially between 400 and 450 and between 650 and 700 Hz. Below 1 kHz the fused sensing only includes the pressure measurements and particle velocity prescription, since the optical data is discarded due to vibration noise. Between 800 and 1100 Hz, the reconstruction is more challenging, and the estimated pressure at the tested reconstruction point fails for the three sensing methods (pressure, optical and the combination). As the wavelength shortens, more acoustic data is required to sample the sound field over space. From 1.1 to 1.8 kHz, the reconstruction achieved by the proposed fused sensing is correct, although some of the modes are shifted towards lower frequencies (see differences between solid gray and black curves in Fig. 2 at 1.5, 1.65 and 1.75 kHz). The fine spatial sampling resolution achieved by the scanning LDV enables to capture the complex spatial features of the sound field in this frequency range (see dashed blue curve in Fig. 2 above 1 kHz). On the other hand, the pressure-based reconstruction fails as the sampling (with $M = 50$ pressure measurements) is not dense enough. Above 1.8 kHz the reconstructed pressure degrades for all three sensing methods.

In order to asses the quality of the reconstruction over space (and not only on a single location), the modal assurance criterion (MAC) was calculated. The MAC is a measure of the spatial similarity between the reference sound field (measured at 110 positions distributed within and around the scanned volume) and the reconstruction. The MAC is defined as $MAC = |\mathbf{p}_r \hat{\mathbf{p}}_r|^2 (\mathbf{p}_r^H \mathbf{p}_r)^{-1} (\hat{\mathbf{p}}_r^H \hat{\mathbf{p}}_r)^{-1}$, where $\mathbf{p}_r \in \mathbb{C}^{R \times 1}$ is the reference sound field ($R = 110$), $\hat{\mathbf{p}}_r \in \mathbb{C}^{R \times 1}$ is the reconstructed pressure, and $(\cdot)^H$ denotes the conjugate transpose. A MAC of 1 indicates perfect spatial similarity between reference and reconstruction. Figure 3 shows the MAC for the three sensing methods (pressure, optical and fused sensing) across frequency. The proposed fused sensing achieves a MAC close to 1 for frequencies below 600 Hz (see solid gray line in Fig. 3), indicating an almost perfect

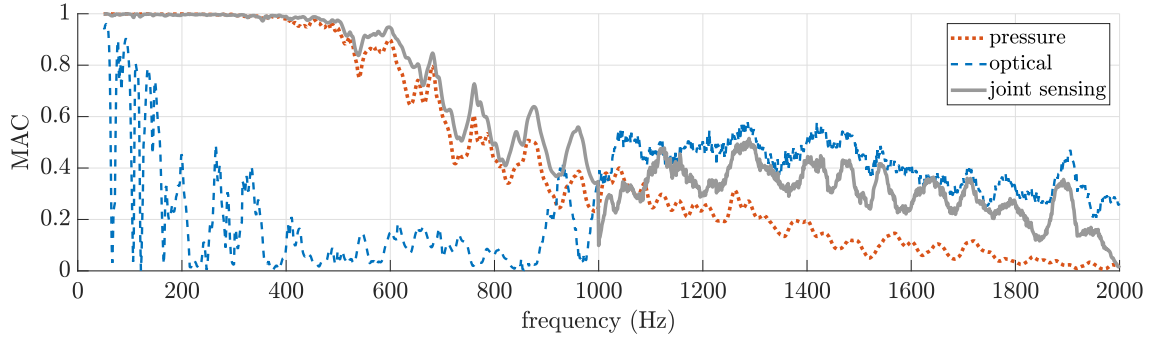


Figure 3: Modal assurance criterion (MAC) across frequency, indicating the spatial similarity between 110 reference pressure measurements and the reconstructed pressure. Dotted red: reconstruction by the pressure measurements exclusively. Dashed blue: reconstruction by the optical measurements exclusively. Solid gray: reconstruction pressure by the proposed fused sensing approach (combines pressure, optical and particle velocity information).

spatial reconstruction. The MAC using only pressure measurements is also high (dotted red line in Fig. 3), while the reconstruction using only the optical measurements fails in this frequency range (dashed blue line in Fig. 3) due to vibration noise. From 600 to 1000 Hz the MAC decreases with frequency for both the fused sensors and the pressure measurements. As the frequency increases the spatial features of the sound field become more complex, with rapid changes of level over space, making the reconstruction more challenging. Nonetheless, the spatial similarity achieved by the fused approach outperforms that of the pressure-based reconstruction. Above 1 kHz the combined measurements archive a MAC of around 0.4, indicating a more accurate reconstruction than using pressure measurements exclusively, and slightly worst reconstruction than using optical measurements exclusively. A spatial reconstruction closer to that of the optical measurements could be obtained by the fused sensing approach by increasing the scaling of the optical measurements in Eq. (7).

4. CONCLUSIONS

In this study we proposed a fused sensing methodology that enables to combine acoustic information acquired by different sensing principles. The proposed framework is used to sample a sound field over space by fusing pressure, optical and velocity measurements. The results indicate improvements in accuracy and an extension of the frequency range in which the reconstruction is correct for the fused approach. This shows the potential of combining acoustic data from different sensing methods to overcome limitations of each specific method and achieve higher accuracy than if the methods were used independently. The methodology presented is also of relevance in other problems where fused sensing data is obtained from different sensors or acquisition systems. The possibility to incorporate prescribed values on the field quantities (in the present study the particle velocity at rigid boundaries) is also significant.

5. ACKNOWLEDGMENTS

The authors would like to thank Salvador Barrera-Figueroa from DFM for letting us the LDV. This study was supported by the VILLUM foundation (grant number 19179).

6. REFERENCES

- [1] M. Park and B. Rafaely, "Sound-field analysis by plane-wave decomposition using spherical microphone array," *J. Acoust. Soc. Am.*, vol. 118, no. 5, pp. 3094–3103, 2005.
- [2] E. Fernandez-Grande, "Sound field reconstruction using a spherical microphone array," *J. Acoust. Soc. Am.*, vol. 139, no. 3, pp. 1168–1178, 2016.
- [3] I. B. Witew, M. Vorländer, and N. Xiang, "Sampling the sound field in auditoria using large natural-scale array measurements," *J. Acoust. Soc. Am.*, vol. 141, no. 3, pp. EL300–306, 2017.
- [4] X. Jia, C. Mattei, and G. Quentin, "Analysis of optical interferometric measurements of guided acoustic waves in transparent solid media," *J. Appl. Phys.*, vol. 77, no. 11, pp. 5528–5537, 1994.
- [5] L. Zipser, H. Franke, E. Olsson, N. Molin, and M. Sjö Dahl, "Reconstructing two-dimensional acoustic object fields by use of digital phase conjugation of scanning laser vibrometry recordings," *Appl. Opt.*, vol. 42, no. 29, pp. 5831–5837, 2003.
- [6] A. R. Harland, J. N. Petzing, and J. R. Tyrer, "Nonperturbing measurements of spatially distributed underwater acoustic fields using a scanning laser doppler vibrometer," *J. Acoust. Soc. Am.*, vol. 115, no. 1, pp. 187–195, 2004.
- [7] Y. Oikawa, M. Goto, Y. Ikeda, T. Takizawa, and Y. Yamasaki, "Sound field measurements based on reconstruction from laser projections," *Proc. IEEE International Conference on Acoustics, Speech and Signal Processing 2005, Philadelphia, PA, USA*, vol. 4.
- [8] Y. Oikawa, T. Hasegawa, Y. Ouchi, Y. Yamasaki, and Y. Ikeda, "Visualization of sound field and sound source vibration using laser measurement method," *Proceedings of 20th International Congress on Acoustics, ICA 2010*, 2010.
- [9] A. Torras-Rosell, S. Barrera-Figueroa, and F. Jacobsen, "Sound field reconstruction using acousto-optic tomography," *J. Acoust. Soc. Am.*, vol. 131, p. 3786, 2012.
- [10] E. Fernandez-Grande, A. Torras-Rosell, and F. Jacobsen, "Holographic reconstruction of sound fields based on the acousto-optic effect," *Proc. Internoise*, 2013.
- [11] R. Malkin, T. Todd, and D. Robert, "A simple method for quantitative imaging of 2d acoustic fields using refracto-vibrometry," *J. Sound Vib.*, vol. 333, pp. 4473–4482, 2014.
- [12] K. Yatabe, K. Ishikawa, and Y. Oikawa, "Acousto-optic back-projection: Physical-model-based sound field reconstruction from optical projections," *J. Sound Vib.*, vol. 394, p. 171, 2017.
- [13] F. Mbailassem, Q. Leclere, E. Redon, and E. Gourdon, "Experimental analysis of acoustical properties of irregular cavities using laser refracto-vibrometry," *Appl. Acoust.*, vol. 130, pp. 177–187, 2018.
- [14] S. A. Verburg and E. Fernandez-Grande, "Acousto-optic sensing of the sound field in a lightly damped room," *Proc. Internoise 2019, Madrid, Spain*.
- [15] S. A. Verburg and E. Fernandez-Grande, "Acousto-optic sensing – spatial reconstruction of the sound field enclosed in a room," *Proc. International Congress on Acoustics 2019, Aachen, Germany*.
- [16] A. Torras-Rosell, "New measurements techniques: Optical methods for characterizing sound fields," *PhD Thesis, Technical University of Denmark*, 2014.

- [17] D. Calvetti and E. Somersalo, *Introduction to bayesian scientific computing*. Springer, 2007.
- [18] P. C. Hansen, *Rank-deficient and discrete ill-posed problems*. Philadelphia: SIAM, 1998.
- [19] E. Fernandez-Grande, F. Jacobsen, and Q. Leclère, “Sound field separation with sound pressure and particle velocity measurements,” *J. Acoust. Soc. Am.*, vol. 132, no. 6, pp. 3818–3825, 2012.
- [20] T. Nowakowski, J. de Rosny, and L. Daudet, “Robust source localization from wavefield separation including prior information,” *J. Acoust. Soc. Am.*, vol. 141, no. 4, pp. 2375–2386, 2017.
- [21] H. Sun and O. Büyüköztürk, “Identification of traffic-induced nodal excitations of truss bridges through heterogeneous data fusion,” *Smart Mater. Struct.*, vol. 24, 2015.